Volume 58(12): 1075–1082, 2010
Journal of Histochemistry & Cytochemistry
http://www.jhc.org

ARTICLE

Localization of Butyrylcholinesterase at the Neuromuscular Junction of Normal and Acetylcholinesterase Knockout Mice

Brigitte Blondet, Gilles Carpentier, Arnaud Ferry, Arnaud Chatonnet, and José Courty

Laboratoire de Recherche sur la Croissance Cellulaire, la Réparation et la Régénération Tissulaires, Université Paris Est, EAC CNRS 7149, Créteil, France (BB,GC,JC); INSERM U974 and Université Paris Descartes, Paris, France (AF); and Département de physiologie animale, Institut National de la Recherche Agronomique, Montpellier, France (AC)

SUMMARY At the mouse neuromuscular junction (NMJ), there are two distinct cholinesterases (ChE): acetylcholinesterase (AChE) and butyrylcholinesterase (BChE). Until now, it has been difficult to determine the precise localization of BChE at the NMJ. In this study, we use a modification of Koelle's method to stain AChE and BChE activity. This method does not interfere with fluorescent co-staining, which allows precise co-localization of ChE and other synaptic molecules at the NMJ. We demonstrate that AChE and BChE exhibit different localization patterns at the mouse NMJ. AChE activity is present both in the primary cleft and in the secondary folds, whereas BChE activity appears to be almost absent in the primary cleft and to be concentrated in subsynaptic folds. The same localization for BChE is observed in the AChE-knockout (KO) mouse NMJ. Collagenase treatment removed AChE from the primary cleft, but not from secondary folds in the wild-type mouse, whereas in the AChE-KO mouse, BChE remains in the secondary folds. After peripheral nerve injury and regeneration, BChE localization is not modified in either normal or KO mice. In conclusion, specific localization of BChE in the secondary folds of the NMJ suggests that this enzyme is not a strict surrogate of AChE and that the two enzymes have two different roles.

(J Histochem Cytochem 58:1075–1082, 2010)

KEY WORDS
butyrylcholinesterase
neuromuscular junction
acetylcholinesterase knockout mouse
cholinesterases inhibitors

TWO DISTINCT cholinesterases (ChE) are located at the neuromuscular junction (NMJ): acetylcholinesterase (AChE) and butyrylcholinesterase (BChE) (Minic et al. 2003). The physiological role of AChE (EC 3.1.1.7.) in nicotinic cholinergic synapses is believed to terminate impulse transmission by rapid hydrolysis of the neurotransmitter acetylcholine (ACh). In contrast, the physiological role of BChE (EC 3.1.1.8.) at the NMJ is still under debate. The currently favored hypothesis regarding the function of BChE is that it acts as a poison scavenger, protecting AChE from inactivation (Duysen et al. 2002).

Advances in mouse genomics offer new approaches for assessing the physiological role of BChE. AChE-knockout (KO) mice have been obtained (Xie et al. 2000) and characterized. Although they do not express AChE, they do express a normal level of BChE (Li et al. 2000; Chatonnet et al. 2003; Adler et al. 2004). AChE-KO mice present a phenotype with many characteristics resembling the cholinergic syndrome seen in wild-type animals poisoned with anticholinesterase agents: they exhibit body tremor, muscle weakness, and susceptibility to seizures (Xie et al. 2000; Duysen et al. 2002; Chatonnet et al. 2003). AChE-KO mice are able to move, breathe, and feed and can survive for several weeks (Li et al. 2000; Xie et al. 2000; Mouisel et al. 2006). However, they exhibit marked altered neuromuscular functioning (Adler et al. 2004; Mouisel et al. 2006). In AChE-KO mice, ACh is likely to be hydrolyzed by BChE and to be slowly removed from the synaptic cleft by diffusion (Adler et al. 2004; Duysen et al. 2007). Additional evidence that BChE functions

Correspondence to: Brigitte Blondet, Laboratoire CRRET, Université Paris-Est, EAC CNRS 7149, 61 avenue du Général de Gaulle, 94010 Créteil, France. E-mail: blondet@univ-paris12.fr

Received for publication May 5, 2010; accepted August 9, 2010 [DOI: 10.1369/jhc.2010.956623].

in vivo to hydrolyze ACh has been provided by AChE-KO mice, which die when BChE activity is inhibited with chlorpyrifos oxon (Duysen et al. 2007), indicating that BChE activity is essential for the survival of AChE-KO mice.

Until now, it has been difficult to obtain information concerning the precise localization of BChE in pre- and postsynaptic elements of the NMJ, mainly due to the lack of selective immunofluorescent markers for BChE. Across the synaptic cleft, the muscle endplate surface is organized into the primary postsynaptic membrane, which contains high concentrations of acetylcholine receptor (AChR) and faces the nerve, and the secondary postsynaptic membrane, which concentrates voltage-gated sodium channels and other molecules and is invaginated, forming the secondary synaptic clefts (Patton 2003).

In this work, we studied ChE localization at the NMJ of normal and KO mice. We used a modification of Koelle's method (Zajicek et al. 1954; Melki et al. 1991) to stain AChE and BChE activity. Light microscope allowed us to directly observe a white precipitate of copper mercaptide at the sites of enzyme activity, avoiding the second step with an ammonium sulphide solution, which leaves a brown deposit consisting of copper sulphide (Zajicek et al. 1954). Under these conditions, ChE cytochemistry does not interfere with fluorescent co-staining, thereby allowing precise co-localization of ChE, AChR, neurofilament, and laminin at the NMJ.

We then addressed the following questions:

Do the localizations of AChE and BChE at the mouse NMJ exhibit a similar pattern? Is BChE localization in the KO mouse NMJ similar to its localization in the wild-type mouse? Does collagenase treatment, which releases matrix-associated enzyme, release ChE from normal or KO mouse NMJ? Are the reasons identical for the high concentrations of AChE and BChE found at the NMJ? Do peripheral nerve injury and regeneration modify BChE localization in wild-type and KO mouse NMJ? Does neuromuscular functioning recovery following nerve injury and regeneration differ in normal and KO mice?

Our hypothesis is that AChE and BChE could be situated at different levels of the synaptic clefts in NMJ, allowing distinct roles for the two enzymes.

Materials and Methods

Animals

All procedures were carried out in accordance with French national and European Union legislation regarding animal experimentation. AChE-KO (Xie et al. 2000) and wild-type mice were provided by the Département de Physiologie Animale of INRA (Montpellier, France), where they were maintained by breeding heterozygous males and females (129/Sv genetic background). The original founders were kindly provided by Dr. O. Lockridge (Eppley Institute; Omaha, NE). Feeding nullizygous mice with an enriched liquid diet (Renutryl 500; Nestlé, Sèvres, France) allowed some animals to survive and pass through the weaning period into adulthood (Duysen et al. 2002). After at least 7 days of acclimatization in the mouse facility at the Faculté des Sciences (Université Paris-Est; Créteil, France), mice aged around 6 weeks were anesthetized with pentobarbital sodium (60 mg/kg) and studied.

ChE Cytochemistry and IHC

The mice were killed, and their levator auris longus (LAL) and gastrocnemius muscles were dissected. LAL muscles are very thin muscles that are commonly used as whole-mount preparation. The gastrocnemius muscle was embedded in Tissue-Tek OCT Compound (Qiagen; Courtaboeuf, France), frozen with dry-ice isopentane, and sectioned at 10 μm in a cryostat. Whole-mount preparations of LAL and cross-sections of gastrocnemius were incubated for 30 min in PBS containing 6% BSA to block nonspecific binding sites. Staining of endplate AChRs was accomplished by incubation (1 hr) with either teramethylrhodamine isothiocyanate-conjugated α-bungarotoxin (10 μg/ml) or Alexa Fluor 488–conjugated α-bungarotoxin (10 μg/ml; Sigma-Aldrich Chimie, St Quentin-Fallavier, France). α-Bungarotoxin binds to the α-subunit of the nicotinic AChR in the NMJ and to α-7 in the central nervous system (Csillik et al. 1999). The preparations and sections were then washed three times in PBS before detection of ChE activity. We used a modification of Koelle's method (Koelle and Friedenwald 1949; Zajicek et al. 1954; Melki et al. 1991) to stain ChE activity. Preparations or sections were preincubated in substrate-free medium for 10 min before incubation at pH 7 (0.1 M phosphate buffer) in the presence of acetylthiocholine iodide (Sigma-Aldrich) for 20 min at 20C. To distinguish AChE from BChE, preincubation and incubation mixtures were supplemented with 10^{-4} M tetraisopropylpyrophosphoramide (iso-OMPA), a selective inhibitor of BChE, or with 5×10^{-5} M 1:5-bis (4-allyldimethylammoniumphenyl)-pentan-3-one dibromide (BW284c51; Sigma-Aldrich), a selective inhibitor of AChE (Feng et al. 1999). Where indicated, sections were treated with highly purified bacterial collagenase (800 U/ml, type VII; Sigma-Aldrich) for 60 min at 37C before staining (Feng et al. 1999).

For IHC, sections were incubated for 1 hr at 20C in the presence of primary antibodies diluted with 1% BSA and 0.4% Triton X-100 in PBS in parallel with α-bungarotoxin. The primary antibodies were anti-NF-200 rabbit polyclonal IgG 1/50 (Sigma-Aldrich) and anti-laminin rabbit polyclonal IgG 1/50 (Sigma-Aldrich). Sections were then washed three times in PBS and incubated for 2 hr with the secondary antibody,

FITC donkey anti-rabbit 1/50 (Interchim; Montluçon, France). Control sections were processed at the same time and in the same way, except that PBS was used instead of the primary antibody. No stained structures were seen in the controls. After three washes in PBS, sections were treated for ChE activity detection. The mounting medium used is Shandon Immu-Mount (Thermo Shandon; Cergy-Pontoise, France).

Digital Imaging Microscopy and Image Analysis Software

Conventional microscopy images were obtained using a CCD monochrome camera (CFW-1310M; Scion; Frederick, MD) fitted to a BH-2 epifluorescence optical microscope (Olympus; Rungis, France) with a C-mount optical adaptor (0.3×). Sequential single image acquisition was obtained from the Scion VisiCapture 2.0 software, using a 40× objective (immersion oil, NA 1.3).

Image processing and original software realizations were accomplished using ImageJ software (Rasband 1997–2010). Co-localization of fluorescent markers and modified Koelle's staining precipitates was made as follows: modified Koelle's staining was imaged by bright field microscopy while maintaining the focal plane used for the fluorescent marker (α-bungarotoxin staining AChR) signal acquisition. The absorbance-encoded image of the transmitted light obtained was inverted and its background was removed. Image panels and apparent co-localization were accomplished using the previously described ImageJ tool (Carpentier 2005; Keller et al. 2007). Staining areas for ChE and AChR were measured using a previously developed fluorescence-labeling segmentation method (Blondet et al. 2002;2006).

Nerve Injury and Neuromuscular Functioning Measurements

In anesthetized wild-type and AChE-KO mice, the right sciatic nerve was exposed and crushed with a fine forceps at the mid-thigh level for 10 sec. The left hind limb served as the control. Fourteen days after nerve injury, we studied in situ isometric tetanic maximal force production in response to nerve stimulation of the tibialis anterior (TA) muscle, as previously described (Mouisel et al. 2006). Mice were anesthetized with pentobarbital sodium (60 mg/kg). The knee and foot were fixed using clamps and pins. The distal tendon of the TA muscle was attached to a force transducer. The sciatic nerve was stimulated upstream of the nerve injury with a bipolar silver electrode, using a supramaximal (10 V) square wave pulse of 0.1 msec duration. All isometric contraction measurements were done at an initial muscle length of L0 (length at which maximal tension was obtained during the twitch). The maximal force was measured during isometric contraction in response to electrical stimulation (frequency 25-150 Hz; duration train 500 msec).

Results

ChE and AChR Localization in Mouse NMJ

ChE cytochemistry was carried out using Koelle's incubation medium, but avoiding ammonium sulphide processing. Cytochemistry without ammonium sulphide treatment did not interfere with AChR staining by fluorescent bungarotoxin, thus allowing precise co-localization of ChE and AChR. Figure 1 shows that ChE staining overlaps AChR staining for gastrocnemius muscle transverse sections (Figures 1B and 1A, respectively, and Figure 1C for a combination of Figures 1A and 1B) and for whole-mounted LAL muscle (Figures 1E, 1D, and 1F).

ChE and AChR staining areas were outlined, and their surfaces were measured (Table 1). The ChE surface area is statistically greater than AChR surface area for gastrocnemius and LAL. Using our staining method, we achieved the comparison of AChR localization (mostly corresponding to postsynaptic membrane in the primary cleft) and ChE localization (primary cleft and secondary folds).

Distinct Localizations for AChE and BChE in Mouse NMJ

To distinguish AChE and BChE activities, we supplemented the reaction mixture either with 10^{-4} M iso-OMPA, a selective inhibitor of BChE, or with 5×10^{-5} M BW284c51, a selective inhibitor of AChE, as described in Materials and Methods. We first demonstrated that no ChE activity was detected in wild-type mouse in the presence of both 10^{-4} M iso-OMPA and 5×10^{-5} M BW284c51 (not shown).

Figure 2 shows a distinct localization for the two enzymes. AChE activity in gastrocnemius (Figure 2B) or LAL (Figure 2H) is localized in the primary cleft and secondary folds (spiny appearance of the borderlines of the AChE-positive gutters). In contrast, BChE activity in gastrocnemius (Figure 2E) and LAL (Figure 2K) exhibits a very different pattern. We did not observe precise co-localization between AChR and BChE (Figures 2F and 2L), even if we were not able to exclude partial overlapping of the two stainings. Instead we observed crystalline linear structures from different orientations, evoking subsynaptic NMJ folds. The crystals observed (in the BChE labeling) correspond to the accumulation of the Koelle's reaction product, in the putative secondary fold regions.

BChE Localization in AChE-KO Mouse NMJ

In AChE-KO mice, ChE activity is exclusively due to BChE. Cytochemistry for ChE (i.e., BChE) activity

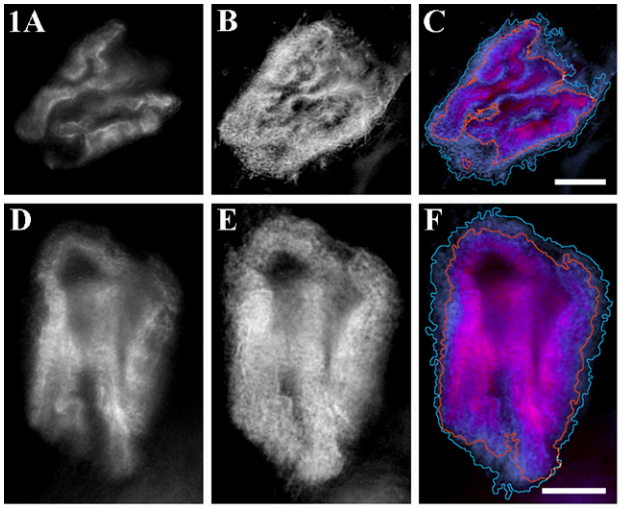

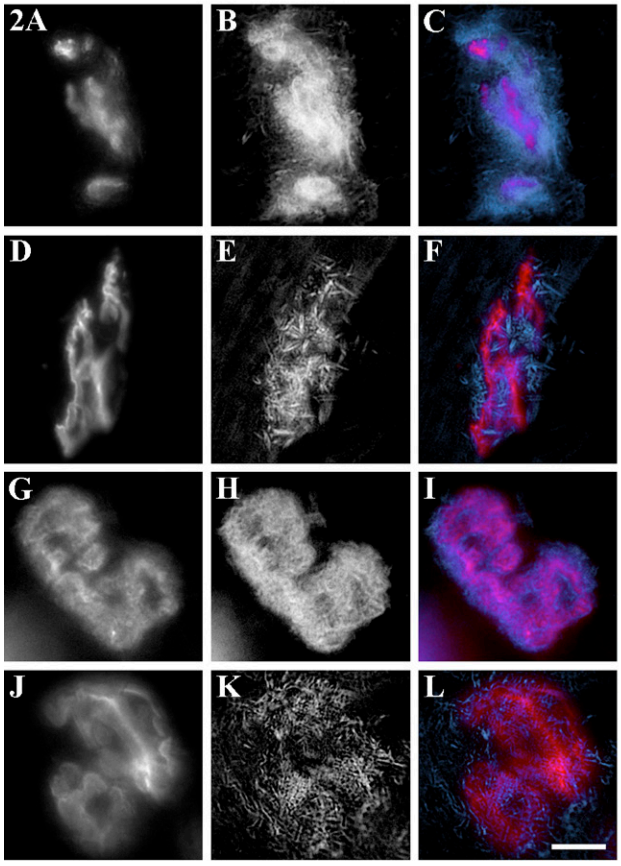

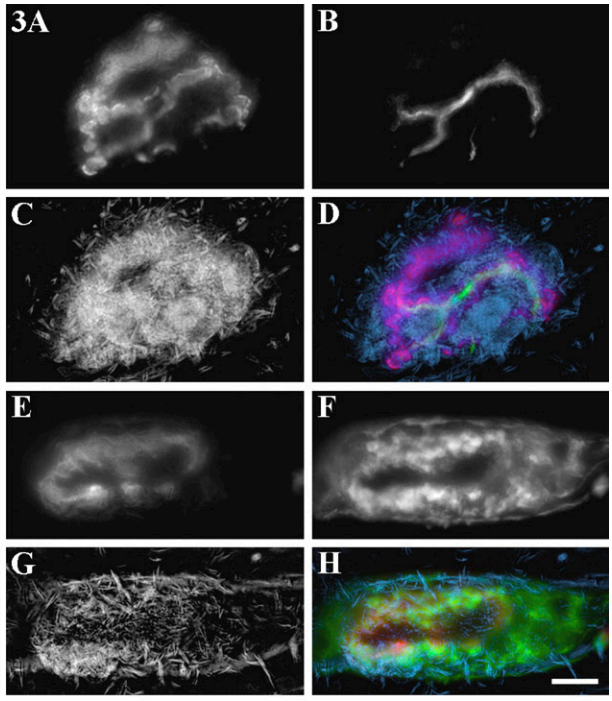

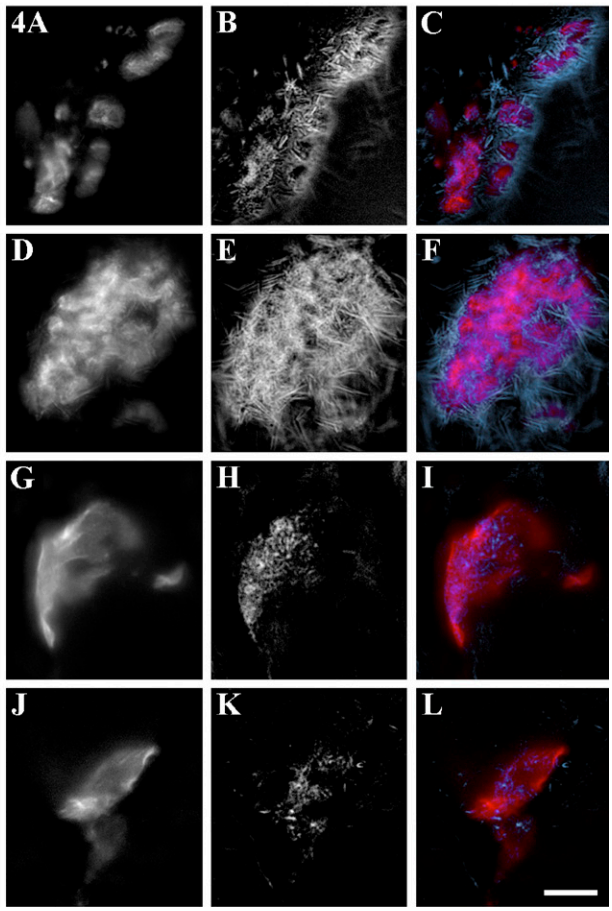

Table 1 Staining areas for ChE and AChR in gastrocnemius cross-sections and whole-mounted LAL muscle

	Gastrocnemius muscle	LAL muscle
ChE area (μm^2)	359.5 ± 33.73 (n=31)	677.2 ± 58.01 (n=14)
AChR area (μm^2)	227.8 ± 24.99 (n=31)	544.5 ± 54.20 (n=14)

ChE, cholinesterase; AChR, acetylcholine receptor; LAL, levator auris longus. Values are means ± SEM. n = number of NMJ analyzed. Statistically significant difference between AChR and ChE areas with $p<0.0001$ in a paired Student t-test for gastrocnemius and LAL muscles.

(blue) was carried out in parallel with differential fluorescent staining (red for AChR and green for neurofilament or laminin; Figure 3) in cross-sections of KO mouse gastrocnemius muscle. BChE localization in mutants (Figures 3C and 3G) is similar to BChE localization in normal mouse (Figure 2E). There was no precise co-localization with AChR (Figures 3D and 3H, red) of linear structures present in the subsynaptic apparatus (Figures 3D and 3H, blue). To precisely situate BChE localization at the mutant motor endplate, axons and motor nerve terminals were stained with anti-neurofilament antibody (Figures 3B and 3D, green) and basal lamina was stained with anti-laminin antibody (Figures 3F and 3H, green). It should be noted that BChE is mainly co-localized with laminin (Figure 3H), thus associated with the subsynaptic apparatus rather than with presynaptic terminals (Figure 3D). However, we cannot exclude a possible localization of the BChE at the presynaptic level.

Effect of Collagenase Pretreatment on AChE in Wild-type Mouse NMJ and on BChE in KO Mouse NMJ

Normal mouse gastrocnemius sections were pretreated with collagenase, which releases matrix-associated enzyme. These sections were then incubated for AChE cytochemistry in Koelle's medium supplemented with 10^{-4} M iso-OMPA (Figures 4A–4C). We observed that AChE was absent from primary cleft and almost exclusively present in crystalline linear structures (Figures 4B and 4C, blue). Collagenase treatment appeared to release AChE from primary cleft but not from junctional folds.

KO mouse gastrocnemius sections were also pretreated with collagenase and incubated in Koelle's medium for BChE cytochemistry (Figures 4D–4F). BChE is present in linear structures (Figures 4E and 4F, blue), and its localization does not differ from that of untreated KO mouse gastrocnemius sections (Figures 2E and 2F, blue). Collagenase treatment does not seem to release BChE from KO mouse NMJ.

BChE Localization in Wild-type and KO Mouse NMJs After Nerve Injury and Regeneration

When peripheral nerve was injured, AChE reappeared after reinnervation at the original sites (Massoulié and Millard 2009). However, it is not yet known whether that is the case for BChE. In previous work (Blondet et al. 2006) analyzing muscle maximal force at different times, we showed that nerve regeneration and

Figures 1–4

Figure 1 Cholinesterases (ChE) and acetylcholine receptor (AChR) localization at the normal mouse neuromuscular junction (NMJ). (**A–C**) Gastrocnemius muscle cross-sections and (**D–F**) whole-mounted levator auris longus (LAL) muscle. The three panels in each row were obtained from the same NMJ, observed in fluorescence after staining with bungarotoxin (**A,D**) or in bright field for Koelle's precipitate (**B,E**). **C** and **F** are composites of both images (red for AChR and blue for ChE). Note that ChE staining overlaps AChR staining. Bar = 10 μm.

Figure 2 Distinct localization for acetylcholinesterase (AChE) and butyrylcholinesterase (BChE) at normal mouse NMJ. (**A–F**) Gastrocnemius muscle cross-sections and (**G–L**) whole-mounted LAL muscle. The three panels in each row were obtained from the same NMJ, observed in fluorescence after staining with bungarotoxin (**A,D,G,J**) or in bright field for Koelle's precipitate (**B,H**, AChE; **E,K**, BChE). **C**, **F**, **I**, and **L** are composites (red for AChR and blue for AChE or BChE). Note the distinct localization of AChE and BChE. Bar = 10 μm.

Figure 3 BChE localization at mutant NMJ. (**A–H**) Knockout (KO) mouse gastrocnemius muscle cross-sections. **A–D** were obtained from the same NMJ, observed in fluorescence after staining with bungarotoxin (**A**), by anti-neurofilament antibody (**B**), or in bright field for Koelle's precipitate (**C**); **D** is a composite of the three images (red for AChR, blue for BChE, and green for neurofilament). **E–H** were obtained from the same NMJ, observed in fluorescence after staining with bungarotoxin (**E**), by anti-laminin antibody (**F**), or in bright field for Koelle's precipitate (**G**); **H** is composite of the three images (red for AChR, blue for BChE, and green for laminin). Bar = 10 μm.

Figure 4 Effect of collagenase pretreatment and nerve injury on ChE localization at normal and KO mouse NMJ. **A–C** were obtained in normal mouse gastrocnemius muscle cross-sections, from the same NMJ after collagenase pretreatment, observed in fluorescence after staining with bungarotoxin (**A**), or in bright field after AChE cytochemistry (in presence of iso-OMPA; **B**). **C** is a composite of both images (red for AChR and blue for AChE). **D–F** were obtained in KO mouse gastrocnemius muscle cross-sections, from the same NMJ after collagenase pretreatment, observed in fluorescence after staining with bungarotoxin (**D**) or in bright field after BChE cytochemistry (**E**). **F** is a composite of both images (red for AChR and blue for BChE). **G–I** were obtained in normal mouse gastrocnemius muscle cross-sections, from the same NMJ 14 days after nerve crush, observed in fluorescence after staining with bungarotoxin (**G**) or in bright field after BChE cytochemistry (in the presence of BW284c51; **H**). **I** is a composite of both images (red for AChR and blue for BChE). **J–L** were obtained in KO mouse gastrocnemius muscle cross-sections, from the same NMJ 14 days after nerve crush, observed in fluorescence after staining with bungarotoxin (**J**) or in bright field after BChE cytochemistry (**K**). **L** is a composite of both images (red for AChR and blue for BChE). Bar = 10 μm.

The Journal of Histochemistry & Cytochemistry

Table 2 Maximal force in response to nerve stimulation and weight of TA muscles 14 days after injury

	Wild-type non-crushed mice (n=8)	Wild-type crushed mice (n=8)	KO non-crushed mice (n=8)	KO crushed mice (n=8)
Maximal force (% of non-crushed mice)	463.4 ± 36.1 (100)	159.5 ± 37.5[a] (35.6 ± 4.5)[a]	130.5 ± 24.4[b] (100)	66.8 ± 14.4[a,b] (50.2 ± 7)[a]
Weight (% of non-crushed mice)	46.3 ± 5.7 (100)	31.9 ± 2.7[a] (68.8 ± 2.7)[a]	30.8 ± 2.8[b] (100)	19.3 ± 1.7[a,b] (63.1 ± 2.1)[a]

[a]Significantly different from non-crushed mice ($p<0.05$).
[b]Significantly different from wild-type mice ($p<0.05$).
TA, tibialis anterior; KO, knockout. Values are mean ± SD. n = number of animals. Groups were compared using two-way ANOVA.

muscle reinnervation are achieved in normal mouse 2 weeks after nerve crush injury. In KO mouse, determination of maximal force (Table 2) allowed us to measure functional recovery.

To localize BChE in the muscle of normal mice 14 days after sciatic nerve crush, ChE cytochemistry was carried out on gastrocnemius cross-sections, using Koelle's incubation medium supplemented with 5×10^{-5} M BW284c51. Nerve injury and regeneration are known to induce synaptic remodeling. We found (Figures 4H and 4I) that localization after crushing is similar to BChE localization in non-crushed mice (Figures 2E and 2F); no precise co-localization with AChR (Figure 4I) and presence of crystalline linear structures (Figures 4H and 4I, blue). For KO mice, cytochemistry was also done 14 days after crushing (Figures 4K and 4L, blue). BChE localization did not exhibit marked differences for BChE in non-crushed normal (Figures 2E and 2F, blue) and KO mice (Figure 3G). It therefore seems that BChE localization is not modified after nerve regeneration in both normal and KO mouse NMJ.

We also studied neuromuscular functioning 14 days after sciatic nerve crush injury. Muscle maximal force in response to nerve stimulation is markedly reduced 2 days following nerve injury (3.3 % of non-crushed muscle). As shown in Table 2, KO and normal mice recovered, respectively, 50.2% and 35.6% of their maximal force. Moreover, recovery of muscle weight was 63.1% in KO and 68.8% in normal mice at 14 days (Table 2). These results indicate that 2 weeks after nerve crush, KO mice are able to partially recover maximal force production and muscle weight, as observed in normal mice.

Discussion

Using a modification of Koelle's method that allowed co-staining of ChE with fluorescent markers and taking advantage of AChE-KO mice, which express only BChE, we have been able to answer the questions addressed earlier.

First, we demonstrate that AChE and BChE exhibit different patterns of localization in normal mouse NMJ. AChE activity is present both in the primary cleft and in the secondary folds, whereas BChE activity appears to be concentrated in structures that evoke subsynaptic folds and almost absent in the primary cleft. The same localization for BChE is observed in KO mouse NMJ. In normal and KO mice, we did not observe precise co-localization between BChE and AChR. It has long been known that AChE is concentrated at extraordinarily high levels in both the primary synaptic cleft and the secondary folds (Couteaux and Taxi 1952; Salpeter 1969; Anglister et al. 1998). Csillik et al. (1999) observed that under the light microscope, the patterns obtained with AChE staining techniques are invariably characterized by the spiny appearance of the borderlines of the AChE-positive gutters. These "spiny" structures, named "organites" by Couteaux (1955), are light microscopic equivalents of the junctional folds (Csillik et al. 1999). We showed that ChE is distributed to a surface area greater than that of AChR. This result has also been described by Martinez-Pena y Valenzuela and Akaaboune (2007).

It has been established that at least part of the endplate AChE is located in the basal lamina (McMahan et al. 1978). The activity observed long ago at the endplate by histochemical methods (Couteaux and Taxi 1952) is mainly due to asymmetric forms of AChE associated with basal lamina (Inestrosa and Perelman 1989; Aldunate et al. 2004; Massoulié and Millard 2009).

To our knowledge, this is the first observation of a specific localization for BChE at the NMJ, and it is different from AChE localization. Several authors (Li et al. 2000; Minic et al. 2003; Girard et al. 2007) have shown BChE staining at the endplate of normal or KO mice, but the method used did not indicate the precise localization of the enzyme. Using our modified Koelle's method, we precisely localized AChR stained with fluorescent bungarotoxin and BChE activity in the same NMJ. BChE activity appears as needle-shaped crystals, which, in conformity with the theories of Koelle, are regarded as being Cu thiocholine (Zajicek et al. 1954). Our results showed that in normal animals after AChE inhibition and in KO mice, these crystals are nearly absent from the primary postsynaptic membrane of the NMJ (identical with the crests of the postsynaptic membrane), which is stained by bungarotoxin. In contrast, they are present in structures that appear to be folds of the secondary postsynaptic membrane.

Second, BChE localization in KO mouse NMJ appears identical to BChE localization in normal mouse NMJ. We did not find precise co-localization of BChE

with AChR, and BChE appears to be associated with synaptic folds. It has been established that BChE activity and distribution in KO mice were not affected by deletion of the *AChE* gene (Li et al. 2000; Chatonnet et al. 2003; Adler et al. 2004). There was no increase in the level of BChE activity to compensate for the lack of AChE activity in KO mice.

Third, in normal mouse, collagenase treatment, which releases matrix-associated enzyme, seems to release AChE from the primary cleft of the NMJ, but not from junctional folds. Collagenase treatment in KO mouse does not affect BChE localization at NMJ: BChE is still present in folds of the secondary cleft.

Much of the AChE in the NMJ occurs in forms that have been called asymmetric (Massoulié and Bon 1982). Synaptic AChE is stably associated with the basal lamina, which runs between the motor nerve terminal and the postsynaptic membrane at the NMJ (McMahan et al. 1978; Sanes and Hall 1979). The collagen tail of asymmetric AChE is likely to be critical for anchoring the enzyme to the basal lamina (Vigny et al. 1983; Rotundo et al. 1998). However, the molecular mechanism or mechanisms underlying its attachment at sites of nerve–muscle contact are still poorly understood (Rotundo et al. 2008).

Moreover, some synaptic AChE may be globular (Anglister et al. 1994), and some asymmetric AChE is found extra-synaptically (Sketelj and Brzin 1985; Blondet et al. 1986).

Our results show that after collagenase treatment, AChE is still present in secondary folds of the NMJ. These results may indicate that some synaptic AChE, especially in secondary folds, is not collagen-tailed.

Concerning BChE, we showed that collagenase treatment did not remove the enzyme from its localization in KO mouse NMJ; BChE remained in secondary folds. Similarly, Li et al. (2000) showed that treatment of crude muscle homogenates with collagenase did not release BChE activity in AChE-KO mice. They concluded that there is a different molecular basis for the high concentrations of AChE and BChE at the murine motor endplate. It seems unlikely that a collagen-tailed form of BChE is highly abundant at the NMJ or is upregulated in the absence of AChE.

Fourth, we showed that BChE localization 14 days after nerve injury and regeneration is not modified in both normal and KO mouse NMJ. It is well known that following peripheral nerve injury, motor axons regenerate to form new NMJ at the original synaptic sites (Ramon Y Cajal 1928; Sanes 2003). Moreover, if denervation induces the disappearance of collagen-tailed AChE, AChE reappears after reinnervation at the original sites (Massoulié and Millard 2009). Concerning BChE, Feng et al. (1999) show that denervation had little effect on BChE at normal mouse NMJ. These results are in agreement with our observation of an unchanged localization for BChE at normal mouse NMJ after nerve injury and regeneration.

In addition, we showed that both wild-type and KO mice exhibit the same recovery for muscle weight and maximal force production in response to nerve stimulation after nerve injury, suggesting that KO mice are able to regenerate their axons and form functional NMJs.

In conclusion, the most important contribution of our study is the observation of a specific localization for BChE in the subsynaptic folds of the NMJ, whereas it is scarcely present in the primary cleft. BChE present in subsynaptic folds may contribute to the hydrolysis of ACh and serves as a backup for AChE.

It should be noted that inhibition of AChE in normal mouse NMJ increases the maximal height and slope of the endplate potential (Minic et al. 2003), but inhibiting BChE does not change the shape of the potential. Following inhibition of AChE or in KO mice that do not express AChE, inhibition of BChE has no effect on the shape of the endplate potential. This suggests that BChE does not hydrolyze the ACh that is active on receptors (Girard et al. 2007). However, BChE inhibition decreases the probability of ACh release by the motoneuron (Minic et al. 2003). It has been suggested that BChE is localized in perisynaptic Schwann cells and that the role of BChE at the NMJ would be to protect nerve terminals from an excess of ACh (Girard et al. 2007). Another explanation for these results is that the two enzymes, AChE and BChE, do not hydrolyze the same pool of ACh. This could result from the fact that these two enzymes are situated at different levels of the synaptic clefts. AChE is mainly located in the primary cleft in regions overlapping the receptor, which would limit the duration of action of ACh. BChE is situated in secondary folds in the periphery of the active zone, which would eliminate ACh that spilled over the active zone. The secondary folds would serve as a sink for excess ACh that is to be hydrolyzed, and the choline produced would be available for recapture by the motoneurone. The different localization of AChE and BChE could also act on different pools of ACh acting on different muscarinic receptors, which have opposite presynaptic functions in modulating quantal ACh release. Nevertheless, the specific localization of BChE in the secondary folds of the NMJ suggests that this enzyme is not a strict surrogate of AChE and that the two enzymes have two distinct roles.

Literature Cited

Adler M, Manley HA, Purcell AL, Deshpande SS, Hamilton TA, Kan RK, Oyler G, et al. (2004) Reduced acetylcholine receptor density, morphological remodeling, and butyrylcholinesterase activity can sustain muscle function in acetylcholinesterase knockout mice. Muscle Nerve 30:317–327

Aldunate R, Casar JC, Brandan E, Inestrosa NC (2004) Structural and functional organization of synaptic acetylcholinesterase. Brain Res Brain Res Rev 47:96–104

Anglister L, Eichler J, Szabo M, Haesaert B, Salpeter MM (1998) 125I-labeled fasciculin 2: a new tool for quantitation of acetylcholinesterase densities at synaptic sites by EM-autoradiography. J Neurosci Methods 81:63–71

Anglister L, Haesaert B, McMahan UJ (1994) Globular and asymmetric acetylcholinesterase in the synaptic basal lamina of skeletal muscle. J Cell Biol 125:183–196

Blondet B, Carpentier G, Ait-Ikhlef A, Murawsky M, Rieger F (2002) Motoneuron morphological alterations before and after the onset of the disease in the wobbler mouse. Brain Res 930:53–57

Blondet B, Carpentier G, Ferry A, Courty J (2006) Exogenous pleiotrophin applied to lesioned nerve impairs muscle reinnervation. Neurochem Res 31:907–913

Blondet B, Rieger F, Gautron J, Pincon-Raymond M (1986) Difference in the ability of neonatal and adult denervated muscle to accumulate acetylcholinesterase at the old sites of innervation. Dev Biol 117:13–23

Carpentier G (2005) 3FluoLabelling Exploring Tools for ImageJ. http://rsb.info.nih.gov/ij/macros/tools/3FluoLablelingExploringTools.txt

Chatonnet F, Boudinot E, Chatonnet A, Taysse L, Daulon S, Champagnat J, Foutz AS (2003) Respiratory survival mechanisms in acetylcholinesterase knockout mouse. Eur J Neurosci 18:1419–1427

Couteaux R (1955) Localisation of cholinesterases at neuromuscular junctions. Int Rev Cytol 4:335–376

Couteaux R, Taxi J (1952) Distribution of the cholinesterase activity at the level of the myoneural synapse. C R Hebd Seances Acad Sci 235:434–436 (in Undetermined Language)

Csillik B, Nemcsok J, Chase B, Csillik AE, Knyihar-Csillik E (1999) Infraterminal spreading and extrajunctional expression of nicotinic acetylcholine receptors in denervated rat skeletal muscle. Exp Brain Res 125:426–434

Duysen EG, Li B, Darvesh S, Lockridge O (2007) Sensitivity of butyrylcholinesterase knockout mice to (–)-huperzine A and donepezil suggests humans with butyrylcholinesterase deficiency may not tolerate these Alzheimer's disease drugs and indicates butyrylcholinesterase function in neurotransmission. Toxicology 233:60–69

Duysen EG, Stribley JA, Fry DL, Hinrichs SH, Lockridge O (2002) Rescue of the acetylcholinesterase knockout mouse by feeding a liquid diet; phenotype of the adult acetylcholinesterase deficient mouse. Brain Res Dev Brain Res 137:43–54

Feng G, Krejci E, Molgo J, Cunningham JM, Massoulié J, Sanes JR (1999) Genetic analysis of collagen Q: roles in acetylcholinesterase and butyrylcholinesterase assembly and in synaptic structure and function. J Cell Biol 144:1349–1360

Girard E, Bernard V, Minic J, Chatonnet A, Krejci E, Molgo J (2007) Butyrylcholinesterase and the control of synaptic responses in acetylcholinesterase knockout mice. Life Sci 80:2380–2385

Inestrosa NC, Perelman A (1989) Distribution and anchoring of molecular forms of acetylcholinesterase. Trends Pharmacol Sci 10:325–329

Keller A, Peltzer J, Carpentier G, Horvath I, Olah J, Duchesnay A, Orosz F, et al. (2007) Interactions of enolase isoforms with tubulin and microtubules during myogenesis. Biochim Biophys Acta 1770:919–926

Koelle GB, Friedenwald JA (1949) A histochemical method for localizing cholinesterase activity. Proc Soc Exp Biol Med 70:617–622

Li B, Stribley JA, Ticu A, Xie W, Schopfer LM, Hammond P, Brimijoin S, et al. (2000) Abundant tissue butyrylcholinesterase and its possible function in the acetylcholinesterase knockout mouse. J Neurochem 75:1320–1331

Martinez-Pena y Valenzuela I, Akaaboune M (2007) Acetylcholinesterase mobility and stability at the neuromuscular junction of living mice. Mol Biol Cell 18:2904–2911

Massoulié J, Bon S (1982) The molecular forms of cholinesterase and acetylcholinesterase in vertebrates. Annu Rev Neurosci 5:57–106

Massoulié J, Millard CB (2009) Cholinesterases and the basal lamina at vertebrate neuromuscular junctions. Curr Opin Pharmacol 9:316–325

McMahan UJ, Sanes JR, Marshall LM (1978) Cholinesterase is associated with the basal lamina at the neuromuscular junction. Nature 271:172–174

Melki J, Blondet B, Pincon-Raymond M, Dreyfus P, Rieger F (1991) Generalized molecular defects of the neuromuscular junction in skeletal muscle of the wobbler mutant mouse. Neurochem Int 18:425–433

Minic J, Chatonnet A, Krejci E, Molgo J (2003) Butyrylcholinesterase and acetylcholinesterase activity and quantal transmitter release at normal and acetylcholinesterase knockout mouse neuromuscular junctions. Br J Pharmacol 138:177–187

Mouisel E, Blondet B, Escourrou P, Chatonnet A, Molgo J, Ferry A (2006) Outcome of acetylcholinesterase deficiency for neuromuscular functioning. Neurosci Res 55:389–396

Patton BL (2003) Basal lamina and the organization of neuromuscular synapses. J Neurocytol 32:883–903

Ramon Y Cajal S (1928) Degeneration and Regeneration of the Nervous System. New York, Oxford press, 265–280

Rasband WS (1997–2010) ImageJ. Bethesda, MD, National Institutes of Health. http://rsb.info.nih.gov/ij/

Rotundo RL, Rossi SG, Peng HB (1998) Targeting acetylcholinesterase molecules to the neuromuscular synapse. J Physiol Paris 92:195–198

Rotundo RL, Ruiz CA, Marrero E, Kimbell LM, Rossi SG, Rosenberry T, Darr A, et al. (2008) Assembly and regulation of acetylcholinesterase at the vertebrate neuromuscular junction. Chem Biol Interact 175:26–29

Salpeter MM (1969) Electron microscope radioautography as a quantitative tool in enzyme cytochemistry. II. The distribution of DFP-reactive sties at motor endplates of a vertebrate twitch muscle. J Cell Biol 42:122–134

Sanes JR (2003) The basement membrane/basal lamina of skeletal muscle. J Biol Chem 278:12601–12604

Sanes JR, Hall ZW (1979) Antibodies that bind specifically to synaptic sites on muscle fiber basal lamina. J Cell Biol 83:357–370

Sketelj J, Brzin M (1985) Asymmetric molecular forms of acetylcholinesterase in mammalian skeletal muscles. J Neurosci Res 14:95–103

Vigny M, Martin GR, Grotendorst GR (1983) Interactions of asymmetric forms of acetylcholinesterase with basement membrane components. J Biol Chem 258:8794–8798

Xie W, Stribley JA, Chatonnet A, Wilder PJ, Rizzino A, McComb RD, Taylor P, et al. (2000) Postnatal developmental delay and supersensitivity to organophosphate in gene-targeted mice lacking acetylcholinesterase. J Pharmacol Exp Ther 293:896–902

Zajicek J, Sylven B, Datta N (1954) Attempts to demonstrate acetylcholinesterase activity in blood and bone-marrow cells by a modified thiocholine technique. J Histochem Cytochem 2:115–121

The Journal of Histochemistry & Cytochemistry